

Tectonic Setting of the Kadiri Schist Belt, Andhra Pradesh, India

Sukanta GOSWAMI*, Pradeep K. UPADHYAY, Purnajit BHATTACHARJEE and
Malaiaindi G. MURUGAN

Atomic Minerals Directorate for Exploration and Research Department of Atomic Energy, India

Abstract: Plate tectonic activity has played a critical role in the development of petrotectonic associations in the Kadiri schist belt. The calc alkaline association of basalt, andesite, dacite and rhyolite (BADR) is the signature volcanic rock suite of the convergent margin. The N-S belt has gone below the unconformity plane of Cuddapah sediments. In the northern part geochemical and structural attributes of the Kadiri greenstone belt is studied along with microscopic observations of selected samples. Harker diagram plots of major elements generally indicate a liquid line of descent from a common source, such that BADR rocks are derived from a common parent magma of basaltic to andesitic composition. These calc-alkaline volcanic rocks are formed at convergent margins where more silicic rocks represent more highly fractionated melt. All the litho-units of this greenstone belt indicate crush and strain effects. The stretched pebbles in the deformed volcanic matrix with tectonite development along with associated greenschist facies metamorphism, alteration and hydration is remarkable. Flow foliation plane with N-S strike and very low angle (5° to 10°) easterly dip and N-S axial planar schistosity formed due to later phase isoclinal folding can be clearly identified in the field. Basic intrusives are quite common in the surrounding area. All the observations including the field setting and geochemistry clearly demonstrate ocean-continent subduction as the tectonic environment of the study area.

Key words: Kadiri schist belt, Tectonics, Unconformity contact, Ocean-continent subduction, Andhra Pradesh, Cuddapah basin, Greenstone belt

1 Introduction

Among the different Archaean granite greenstone terranes of the eastern block of Dharwar Craton in India, the most unique is the Kadiri schist belt, which is dominated by acid volcanics with relatively minor proportions of metabasalt and meta-andesite. However, despite a number of publications available on granitoids adjoining the Kadiri schist belt, metavolcanics of the schist belt have not yet been attempted properly. The origin and tectonic setting of surrounding granitoids cannot be regarded as independent of the metavolcanics within the belt. This paper is intended to fill the gap and to characterize the schist belt rocks.

The schist belt rocks have undergone low grade greenschist facies metamorphism. The northern extension of the Kadiri schist belt, which has gone below the unconformity plane defined by overlying sediments of Cuddapah basin (Fig. 1), has been demarcated near

Damanapalle village, Anantapur district, Andhra Pradesh (Toposheet No. 57J/3). The greenstone belt litho-units comprise dominantly acid volcanic, namely rhyolite, dacite, and rhyodacite, along with andesite and metabasalt. The sequence of flows are found to occur just like bedding planes with N-S strike, 5° to 10° = >E dip (Fig. 2). Sub-rounded volcanic bombs (with diameters > 64 mm) and lapilli (2 to 64 mm) are embedded within the acid volcanic flow (Fig. 3) found near the unconformity contact. Extensively recrystallized and altered dark fine grained matrix, stretched N-S elongated quartzo-feldspathic clasts found along the belt (Fig. 4) are probably formed by dynamothermal metamorphism related to strong non-uniform stress. The felsic breccias in the Kadiri greenstone succession are characterized by units with broadly lentoid shapes and traced for up to several kilometers along strike. Broken, crushed, rotated grains of quartz along N-S fractures indicates brecciation (Fig. 5a). There are autoclastic fragmental rocks that comprise clasts generated by in-situ fragmentation of coherent magmatic bodies (Fisher and Schmincke 1984; McPhie et al., 1993).

* Corresponding author. E-mail: sukantagoswami.amd@gov.in



Fig. 2. Acid volcanic flows of Kadiri greenstone belt with gentle easterly dipping flow beds near Dorigallu village.

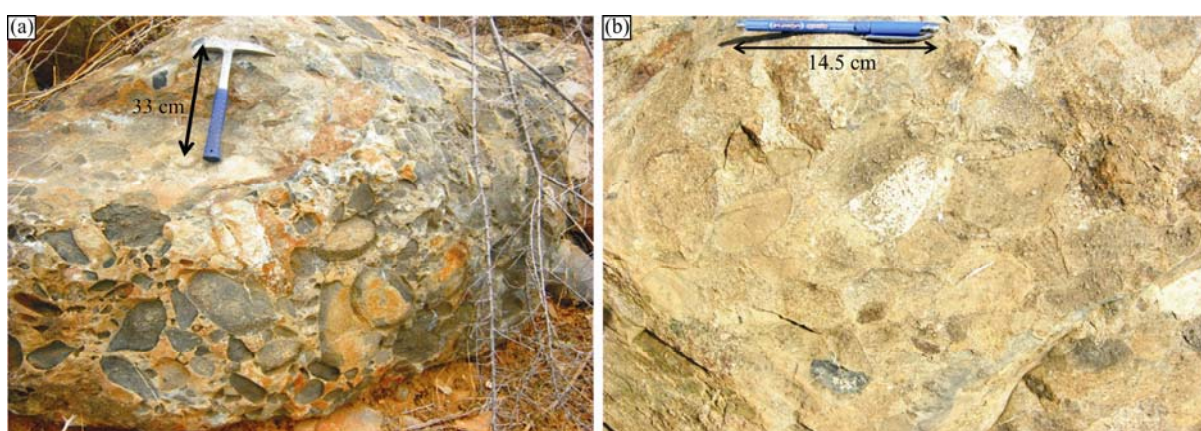


Fig. 3. (a), Coarse pyroclastic deposit composed of a large proportion of sub-rounded, volcanic bombs (predominant grain size >6.4 cm). (b), Lapillistone with 2 to 64 mm average size of more than 75% of the pyroclastic fragments.

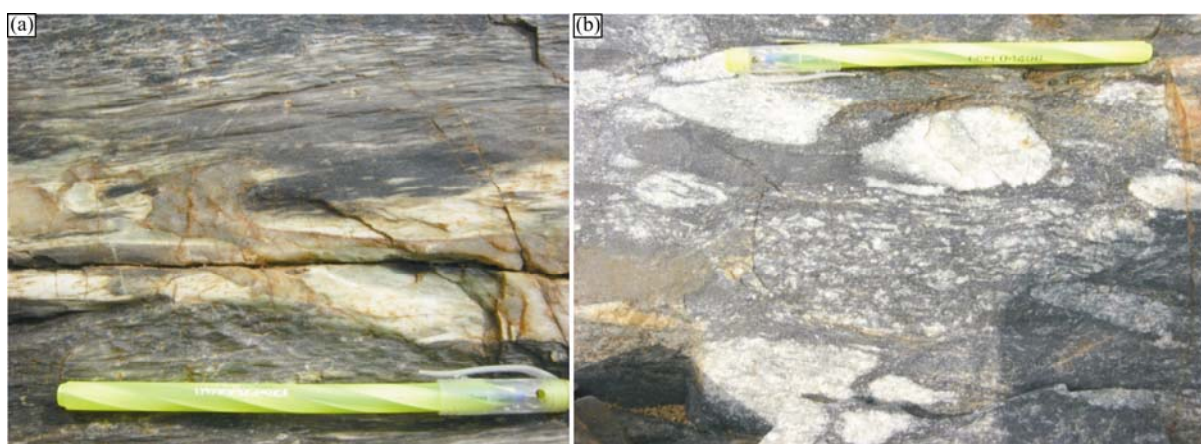


Fig. 4. (a), Acid volcanics with recrystallized and altered dark very fine grained foliated matrix (Pen length 14 cm). (b), Pre-kinematic stretched and N-S elongated quartzo-feldspathic clasts related to strong non-uniform stress.

Autobreccias commonly form on the base and top of lava flows (Fisher and Schmincke, 1984; Cas and Wright, 1988; McPhie et al., 1993). Quartz-rich, more resistant mineral bearing clasts have remained larger in fine volcanic matrix and later foliated due to shearing (Fig. 5b). Field observations indicate the presence of combined cataclastic and intra-crystalline plastic deformation.

Ductilely elongated quartz ribbons and foliated mylonites are indicative of a shear zone (Fig. 6), and N-S foliation occurs regionally. Abundant breccias and agglomerates indicate a fissure vent surrounding environment. Fragments in breccias are chiefly felsic volcanics and range up to 1 m across although generally averaging 10–30 cm. The ratio of pyroclastics to flows increases both



Fig. 5. (a), Broken, crushed, rotated grains in fine acid volcanic matrix (Pen length 14 cm). (b), Pre-kinematic broken grains become lensoidal shaped due to shearing stress and arranged along foliation.

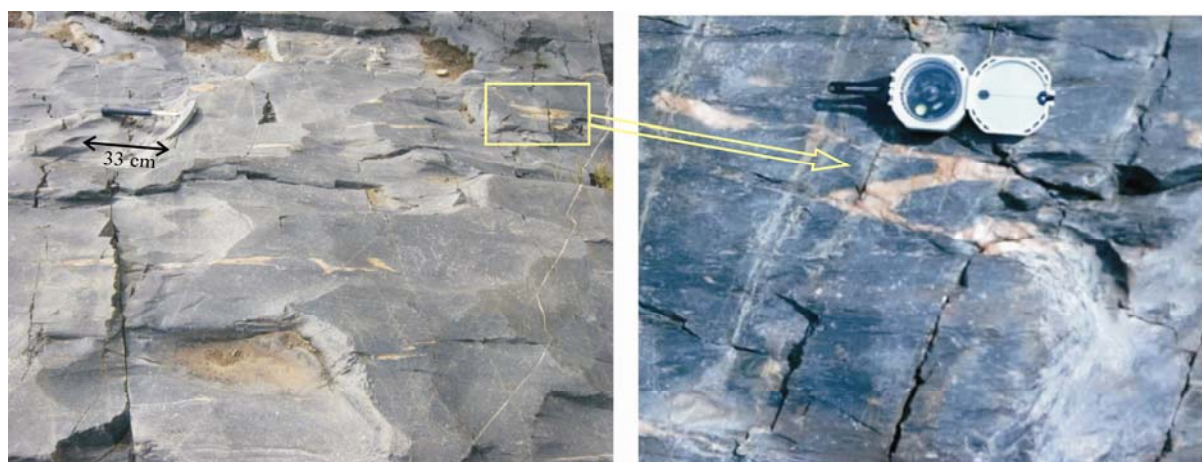


Fig. 6. Ductile elongated quartz ribbons and isoclinal folding, fine foliated mylonites are indicative of brittle ductile shear zone.

with increasing stratigraphic height and with decreasing distance to eruptive centers (Goodwin et al., 1972) and this similar setup suggests that the studied section is in the upper portion of the greenstone succession. Units are poorly sorted and fragments are generally angular although some units are composed of well-rounded fragments (agglomerates). Felsic medium to fine ash-flow tuff units and are generally well bedded. Individual beds range from 1 cm to a few meters thick. The color of these rocks is highly variable depending, in part, on degree of alteration. Gneissic complexes with feebly developed gneissosity comprise the dominant component in the granitic portion of this granite-greenstone terrane and the foliation in the gneissic complexes parallels that in greenstone belts near greenstone-gneiss contacts and becomes exceedingly variable in intervening regions.

Therefore, this paper presents a summary of field observations, petrography, geochemical data and interpretations related to the tectonic setting of the Kadiri schist belt.

2 Geological Setting

The narrow N-S trending linear Kadiri Greenstone Belt

is located to the South West of Cuddapah Basin in the Eastern Dharwar Craton (EDC) covering parts of Anantapur and Chittoor districts, and lies between $N13^{\circ}45'-14^{\circ}7'$ to $E78^{\circ}2'-78^{\circ}15'$, and comes under the survey of India Toposheet Nos. 57 J/3, 57J/4, 57K/1 and 57K/2. The greenstone belt litho-units comprise mainly acid to intermediate metavolcanics and associated sedimentary sequences along with granitic plutons.

The present study area is a NW-SE rectangular block from Peddanagaripalle in the SE to Damanupalle in the NW (Toposheet No. 57 J/3), covering basement granitoids, schist, basic intrusives, quartz reefs and cover sediments of the Gulcheru Formation. The nonconformity contact between basement and Gulcheru quartzite runs along a NNW-SSE trend (Fig. 1). The granitoids are found to represent two different categories: 1. dark gray colored coarse grained hornblende-biotite granite with feeble gneissosity at places occupying relatively flat peneplains; 2. medium to coarse grained granodiorite of pink to gray colour found in hillocks intruded over the peneplains. This pink granodiorite occurs as plutons. The mafic component is found to increase gradually near the contact areas with basic intrusives and the schist belt. Several fracture trends are marked along E-W, NE-SW and NW-SE and N-S

directions. However, NE-SW and E-W trending fractures are more dominant. Regional schistosity and gneissosity shows a N-S trend in the schist belt and gneisses. Younger granitic intrusions are also found to occur along N-S. The granitoids are intruded by basic intrusions along NW-SE, NE-SW, WNW-ESE and ENE-WSW trends. The contact zones are sharp and mylonitization of basic rocks with mylonitic foliation and very fine grain size reduction along with smooth soapy surface development is common. The granitoids were defined as tonalite-trondhjemite-granodiorite gneiss, tonalite-granodiorite-monzogranite and monzogranite-syenogranite (Sreenivasulu et al., 2014; Nandy et al., 2013). The greenstone belt litho-units comprise dominantly acid volcanics namely quartz porphyry, quartz-feldspar porphyry and rhyolites with comparatively lesser basic volcanics like metabasalts and meta-andesites. All the litho-units of the greenstone belt indicate crush and strain effects in thin sections. Alteration, twinning and zoning of minerals are also seen. Quartz and plagioclase commonly occur as phenocrysts set in a fine-grained matrix of quartz, feldspar, biotite, muscovite, chlorite and epidote. Apatite, sphene and opaques occur as inclusions. The rocks exhibit flow structure, cataclastic texture and crude foliation. In basic volcanics, hornblende, actinolite and plagioclase chlorite, biotite, epidote and quartz are the prominent minerals. Sub-spherical accretionary lapilli made up of aggregated coarser ash, lapilli or aggregates of variable sized clasts (Fig. 7) are common near the unconformity and these are commonly used to indicate magma–water interaction (Wohletz and McQueen, 1984). A generalized section across the Kadiri schist belt can broadly be divided into three units, namely, mixed breccia, tuff and finely banded tuffs which grade upwards into laminated cherty tuffs. The

felsic breccias are characterized by units with broadly lentoid shapes.

3 Structural Setting

The Kadiri schist belt is like other greenstone belts that are invariably subjected to regional scale sinistral shearing, mostly along their eastern contacts, with the granitoids forming major discontinuities and some of them form as late Archaean sutures/terrane boundaries in the EDC (Drury, 1980). Volcanic activity at subduction zones produces abundant fragmental material, referred to as volcaniclastics, owing to the explosive nature of the eruptions and the potential for interaction of magma with water. Lava might have erupted along the N-S linear fracture, or fissure vents, and are of composite type that contain a wide variety of composition ranges from rhyolite to andesite, but they are generally dominated by dacite. Acidic lava typically has higher viscosity, hence spread is limited and more likely to build up around the vent source and probably blocked the pathway of eruption and thus forceful ejection took place along with fracturing and breaking of granitic country rocks, which have given the brecciated pyroclasts of solidified acid lava, quartz vein, granite from wallrock. Other than lapilli with diameter 2–64 mm, pyroclasts with diameter larger than 64 mm are also found to be embedded on the lava (Fig. 3). The broken angular blocks indicate solid fragments and rounded clasts are bomb formed during violent eruption of masses of molten lava which cool into solid fragments before they reach the ground and acquired aerodynamic round shapes during their flight. The differential movement of rock masses in the shear zone is certainly a kinematic event but it has not created a regional tectonic

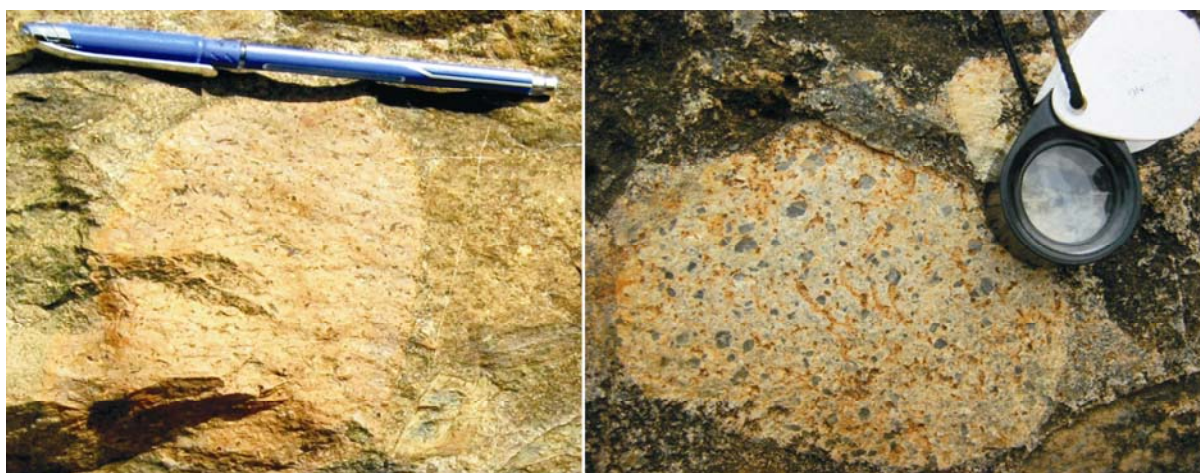


Fig. 7. Sub-spherical accretionary lapilli made up of aggregated coarser ash, lapilli or aggregates of variable sized clasts often seen near unconformity at Damanupalle village and these are commonly indicate magma–water interaction (Pen length 14.5 cm).

event of significance. The porphyroblast–matrix relations were helpful in determination of pre-, syn- and postkinematic fabrics. The clasts that existed in the rock prior to deformation occur within the fine foliated acid volcanic matrix. They exhibit ribbon like appearance, fractured, bent grains and the broken pieces of larger clasts shows matching boundaries like a jigsaw. Syn- to prekinematic signatures are common and indicating metamorphism and deformation might had occurred in unison. The continuous schistosity generated by dynamic recrystallization of aligned grains are a mixture of bent and straight recrystallized grains.

The rocks are deformed with a specific texture and structure that records the deformation by developing the preferred clast orientation. The fabric appears to be a type of tectonite. Foliation development in these rocks is due to $\sigma_1 > \sigma_2 \geq \sigma_3$ stress condition prevailing in the area. Stretched pebbles in the deformed volcanic matrix gives L-S tectonite (Fig. 8) in which the σ_1 is maximum E-W compressive stress, σ_3 is the minimum compression or extension/stretching along N-S and σ_2 is the vertical intermediate stress axis.

Mechanical rotation and elongation of clasts along the preferred N-S direction and the internal deformation and crushing of grains at places by cataclasis during rotation due to E-W compression is noteworthy. The deformation signature corresponds to a shallow low temperature environment of regional metamorphism. Isoclinal folds

with steeply dipping axial planes and moderate to steep plunges are preserved. The cross section through rhyolite lava exhibits flow banding of visually distinct layers of differing crystallinity or vesicularity.

4 Microscopic Analysis

The deformation conditions from the structures in the rocks observed both in the field and under the microscope can be related to the timing and nature of alteration. Along the margin of the greenstone belt the pink granite is found to become highly altered and deformed which has led to granulation of major minerals and fracturing in the rock (Fig. 9). Plagioclase feldspar, quartz, orthoclase and chlorite are the major minerals followed by sphene, epidote and calcite. Phenocrysts of feldspar in a groundmass of fine to medium grained quartz and feldspar is common and fractures are later invaded by altered products like chlorite, calcite, epidote, sphene and opaques. The feldspars have often undergone saussuritization and sericitization. Near the contact with pink granite-acid volcanics forceful intrusion effects are found in the form of xenoliths of granitoids in fine grained matrix. The coarse grained plagioclase feldspar and orthoclase/sanidine are embedded in a groundmass of fine grained quartz and feldspar rich volcanic matrix. These microstructures are indicative of cataclastic flow. Another interesting feature that is also clearly observed in the field

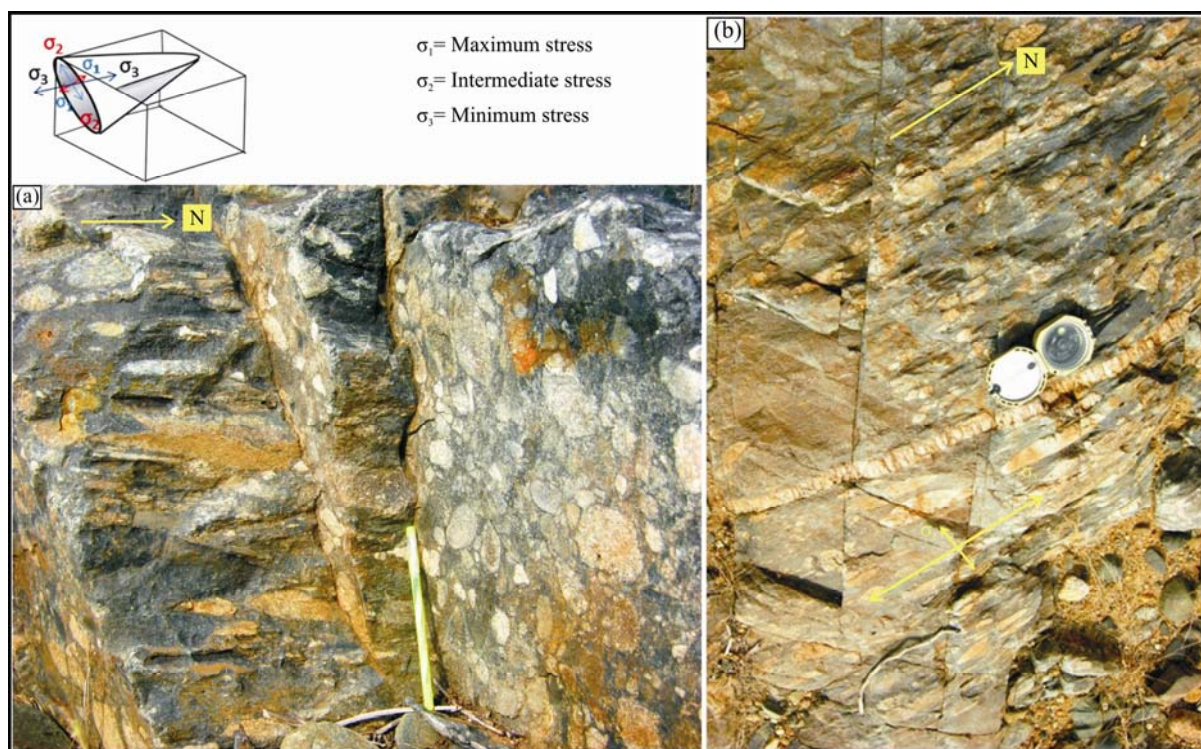


Fig. 8. Stretched pebbles in the deformed volcanic matrix gives L-S tectonite in which the σ_1 is maximum E-W compressive stress, σ_3 is the minimum compression or extension/stretching along N-S and σ_2 is the vertical intermediate stress axis.



Fig. 9. (a). Fractured granite along margin of Kadiri schist belt in hand specimen and microscopic scale. (b), Deformation led to granulation of major minerals and fracturing in the rock; 2X, TL, 1N. (c), Phenocryst of plagioclase and sanidine in fine grained matrix 2X, TL, 2N.

is tectonite development where the prekinematic clasts are found to be broken in lenticular shapes due to shearing and porphyroclasts developed in sheared mylonite with tapered rims of fine grained materials to form augen texture (Fig. 10). The shape of the deformed ϕ -type mantled porphyroclast with symmetrical tails cannot be used as shear sense indicator. However, the studies of most of the outcrop points to a sinistral sense of shearing. Under the microscope are observed very fine grained, foliated acid volcanics composed chiefly of quartz, sericite and chlorite and other flaky clay minerals and titanate minerals with flow foliation (Fig. 11). Epidote, calcite, plagioclase

feldspar and zoisite are the minor to accessory mineral phases. Medium intensity deformation and metamorphism of greenschist facies condition and associated alteration is notable. The pink coloured fracture filled bands are mostly composed of medium grained quartz, microperthite dominantly along with minor epidote, sericite and chlorite (Fig. 12). Some veins are filled with quartz, feldspar and apatite as well (Fig. 13). The alteration of almost all the minerals, like chloritization of biotite and amphibole, sericitization, chloritization and calcitization of plagioclase feldspar, etc., points to hydration.

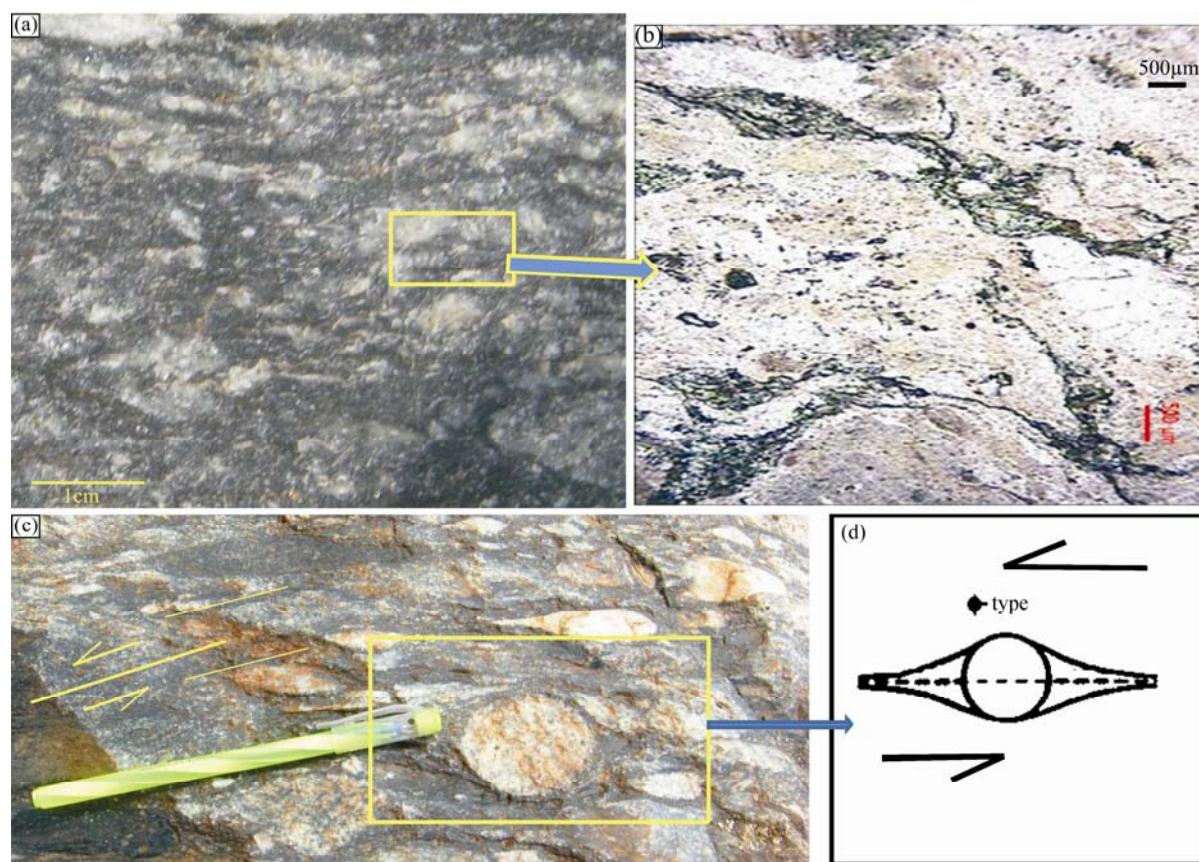


Fig. 10. (a), Sheare planes formed due to ductile deformation and storage of dislocation tangles in response to flow in the matrix; (b), Part of the highly sheared mylonite with augen under microscope, 2X, TL, 1N; (c and d), The mantles are finer grained than porphyroclast core and further deformed by shear to form ϕ -type tails that extend from the porphyroclast in both directions into the mylonitic foliation (Pen size 14 cm).



Fig. 11. (a), Flow foliation represents physical or chemical heterogeneity in the viscous lava which have been sheared out and attenuated by laminar flow during extrusion and deformed into folds with axial planar cleavage development. (b), N-S lineation indicating axial planar foliation (Pen length = 14cm). (c), Alignment of chlorite along flow direction, 10X, TL, 1N.



Fig. 12. Hand specimen of acid volcanics with pink coloured fracture filled bands and corresponding photomicrograph shows dominantly quartz, microperthite along with minor epidote, sericite and chlorite.

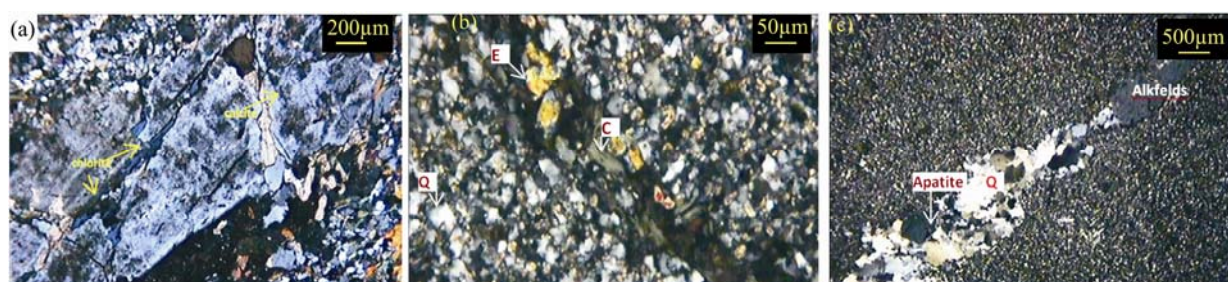


Fig. 13. (a), Phenocryst of feldspar filled with chlorite and calcite, 5X, TL, 2N. (b), Epidote (E), chlorite (C) as minor vein filling component in quartz (Q) rich meta rhyolite 20X, TL, 2N; (c), Quartz, titanate bearing volcanics cut across by fracture filled with quartz apatite and alkali feldspar 2X, TL, 2N.

5 Sample Description and Analytical Methods

UV spectroscopy for SiO_2 , flame photometer for Na_2O , K_2O and inductively coupled plasma optical emission spectroscopy (ICPOES) were used for TiO_2 , Al_2O_3 , MgO , MnO , CaO and P_2O_5 and also for detection of some trace elements like Th, Sr, Ba, Nb, Zr, Cr, V. Atomic absorption spectroscopy (AAS) was used for Fe_2O_3 along with Rb, Cu, Ni, Co. The samples were collected systematically across the schist belt to make out the variation in terms of mineralogy and geochemistry. The standard representative

well preserved outcrops across the Maddileru river section in the south of Dorigallu village is chosen for sampling from east to west. The samples collected across this N-S trending schist belt exhibits bedded tuff, volcanic chert and brecciated welded tuff and acid volcanics. All the representative units are taken into consideration for the study.

Major, minor and trace element concentrations (Table 1) provided information to understand the evolution of the magma. Harker diagrams (after Harker, 1909) display smooth, curvilinear trends for almost all rock data points

Table 1 Major element oxides (wt%), selective minor and trace element (ppm) data of acid volcanics of Kadiri greenstone belt near the unconformity contact with Cuddapah sediments

S.No.	D1	D2	D3	D4	D5	D6	D7
Rock	Kadiri schist/greenstone belt acid volcanics						
SiO ₂	73.71	62.92	72.66	68.91	71.09	62.95	65.96
Al ₂ O ₃	15.14	19.96	15.59	14.43	14.52	14.35	15.48
TiO ₂	0.23	0.36	0.28	0.35	0.17	0.81	0.56
Fe ₂ O ₃	0.46	1.29	0.69	0.01	0.13	0.4	0.6
FeO	1.22	3.31	1.22	3.24	1.8	5.47	3.74
MnO	0.05	0.07	0.06	0.09	0.04	0.11	0.09
MgO	1.41	2.89	1.59	2.51	1.54	2.84	2.5
CaO	0.97	0.93	0.8	3.08	5.13	6.41	2.31
Na ₂ O	2.61	1.63	2.27	3.79	1.18	3.54	4.63
K ₂ O	1.22	2.19	1.4	0.68	0.72	0.39	1.04
P ₂ O ₅	0.11	0.14	0.17	0.3	0.23	0.17	0.29
U ₃ O ₈	0.001	0.002	0.001	0.002	0.003	<0.001	0.001
Ba	765	1110	530	305	190	365	725
Co	<10	15	<10	<10	<10	20	15
Cr	20	75	35	25	60	100	50
Cu	20	15	30	40	15	30	180
Mo	<10	<10	<10	<10	<10	<10	<10
Nb	<10	<10	<10	<10	<10	<10	<10
Ni	10	45	35	20	10	70	25
Pb	<25	<25	<25	25	<25	<25	<25
Rb	50	85	60	30	35	10	25
Sr	370	185	205	505	460	400	370
Th	20	30	20	25	20	25	30
V	25	75	35	40	20	110	70
Zn	35	50	40	85	35	85	50
Zr	100	135	115	120	100	115	135
La	21	44	22	32	30	32	30
Ce	44	83	50	66	59	55	64
Pr	<5	6	<5	<5	<5	<5	5
Nd	18	36	23	28	25	32	30
Sm	<5	<5	<5	<5	<5	<5	<5
Eu	0.7	1.8	0.9	1	0.9	1.4	1.2
Gd	<2	4	2	3	2	4	3
Tb	<2	<2	<2	<2	<2	<2	<2
Dy	<2	3	2	2	2	3	2
Ho	<2	<2	<2	<2	<2	<2	<2
Er	<2	<2	<2	<2	<2	<2	<2
Tm	<2	<2	<2	<2	<2	<2	<2
Yb	<1	1.3	<1	<1	<1	1.6	1.2
Lu	<1	<1	<1	<1	<1	<1	<1
Sc	<1	3	1	2	<1	8	3
Y	6	15	9	12	10	18	13

and indicate genetically related rock types with in the schist belt (Fig. 14). Major element variations reflect a liquid line of descent from a common source in which diversification caused major elements to either increase or decrease progressively with respect to variations in weight percent SiO₂. The parent magma from which the rocks are derived has a composition near that of the sample with the least SiO₂, that is of andesitic composition. As predicted by Bowen's reaction series, MgO and FeO decrease with increasing SiO₂. Upon fractionation, calc-alkaline magmas record a progressive decrease in iron and magnesium with increasing SiO₂ and alkali concentrations. Available FeO and MgO are progressively removed from the melt through crystallization of olivine, pyroxenes, amphiboles, biotite and iron oxide minerals such as magnetite. The removal of ferromagnesian minerals enriches the melt in Na₂O, K₂O and SiO₂. The SiO₂ vs FeO/ MgO plot

(Miyashiro, 1974) of data points fall in the calc-alkaline field (Fig. 15). Thus, with increasing fractionation from magma, the calc-alkaline series exhibits increases in SiO₂, Na₂O and K₂O and decreases in CaO, MgO and total iron (Bowen, 1928; Miyashiro, 1974; Grove and Kinzler, 1986). However, due to successive metamorphism and alterations the addition or removal of certain oxides can show some discrepancy. The alteration indices also have been calculated. Chemical Index of Alteration (CIA) ranges from 58 to 80, indicating moderate to high intensity of chemical weathering and removal of labile cations like Na₂O and K₂O. Ishikawa Alteration Index (IAI) (Ishikawa et al., 1976) to quantify the intensity of sericite and chlorite alteration suggest low degree of alteration ranges from 24 to 66. As far as tectonic setting is concerned, the data suggest a convergent plate margin (Fig. 16) wherein batholiths and composite volcanoes develop above the subduction zone. Spider diagrams used to demonstrate the enrichment or depletion of compatible versus incompatible elements, LREE versus HREE variation that may indicate diversification trends or magmatic source. The trace element concentrations of the samples are most similar to OIB (Fig. 17a). LREE and the largest LIL are enriched relative to HREE in a way somewhat similar to E - MORB (Fig. 17b) and highly dissimilar to N - MORB (Fig. 17c). The Kadiri greenstone volcanics are between 10 and 100 times more enriched in LIL and LREE compared to the primitive mantle (Fig. 17d). It is likely that the parent melts for the acid volcanics were produced by partial melting of a relatively undepleted mantle source. The progressive changes in chemical composition are plotted on a triangular AFM (A, alkali; F, iron; M, magnesium) diagram (Fig. 18) and studied along with Harker diagrams to demonstrate that the calc-alkaline rocks were generated by diversification of andesitic parent magma. The submarine volcanism along fissures developed in the convergent plate boundary involved the transfer of magma (together with phenocrysts, dissolved volatiles, and country-rock material entrained from the conduit walls or ground surface) from some depth onto the surface.

6 Discussion

East Dharwar craton have Mesoarchaeon and Palaeoarchaeon crust in the east (Dey et al., 2014) and TTG (Tonalite-Trondhjemite-Granodiorite) gneiss is an important component like any other craton (Shan et al., 2016). The convergent margin magmatism affected by a number of variables and finally eroded volcanic arc materials are deposited as volcanoclastics in the back arc basin just like another case of the Ramagiri schist belt W to the Kadiri terrain (Goswami et al., 2016).

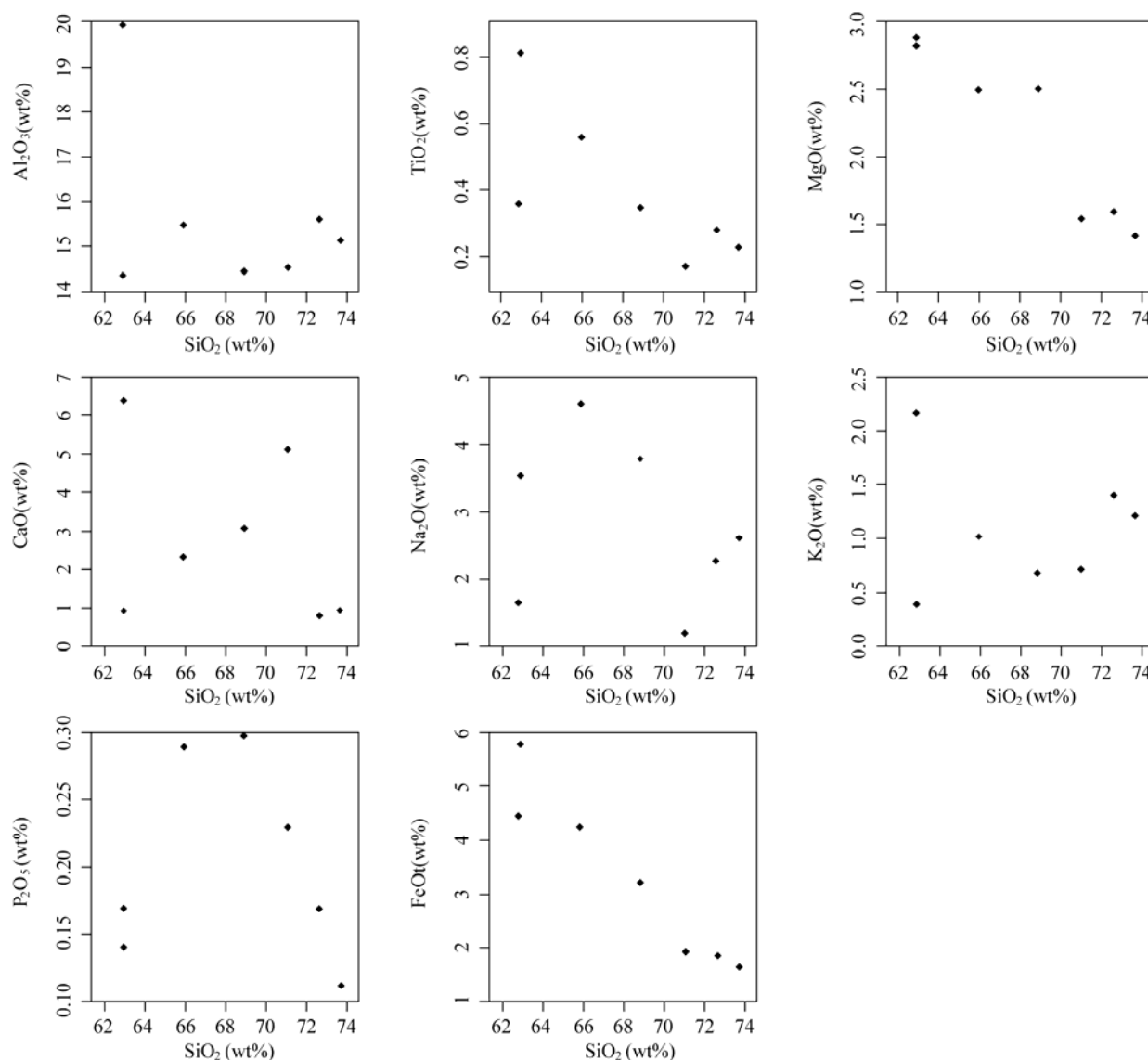


Fig. 14. Harker diagram shows variation of different major element oxides with reference to SiO_2 .

The published isotopic/age data on the Neoarchean greenstone belts of the Dharwar craton have suggested two main episodes of greenstone volcanism in the Neoarchean at 2.7–2.65 Ga and 2.58–2.55 Ga and interpreted time relationship of felsic volcanics with mafic volcanics, surrounding TTG plutons. In the Dharwar craton, 2.7 Ga volcanism was dominated by mafic lavas, whereas 2.6–2.54 Ga volcanism was dominated by intermediate and particularly felsic lavas (Jayananda et al., 2013). The 2.7 Ga episode of greenstone volcanism is contemporaneous with emplacement of TTG suites surrounding the greenstone belts. The 2.58–2.54 Ga felsic volcanism is coeval with, and potentially genetically linked to, widespread juvenile calc-alkaline magmatism and crustal reworking throughout the EDC (Chadwick et al., 2007; Chardon et al., 2008, 2011). The two episodes of volcanism and associated plutonism correspond to two

crustal accretion events contributing to continental growth of the EDC and reworking of the eastern fringe of the WDC (Jayananda et al., 2006; Chardon et al., 2008, 2011). Jayananda et al. (2013) have presented the 2556 ± 13 Ma age of the felsic volcanics of the Kadiri schist belt by U–Pb SIMS which are interpreted as the crystallization age of the felsic magmas. According to Chadwick et al. (2000), EDC can be regarded as a calc-alkaline arc granitoid batholith with accreted segments of intervening narrow linear greenstone belts of inner arc type, which along with intrusive synkinematic granitoids finally accreted on to the western block of Dharwar Craton. The calc-alkaline trend with ocean-continent convergence setting of the present data supports the observation of Chadwick et al. (2000).

With rising towards the surface, the water vapor might have exsolved as a separate phase from the magma. Exsolution of gas generated expanding gas bubbles and

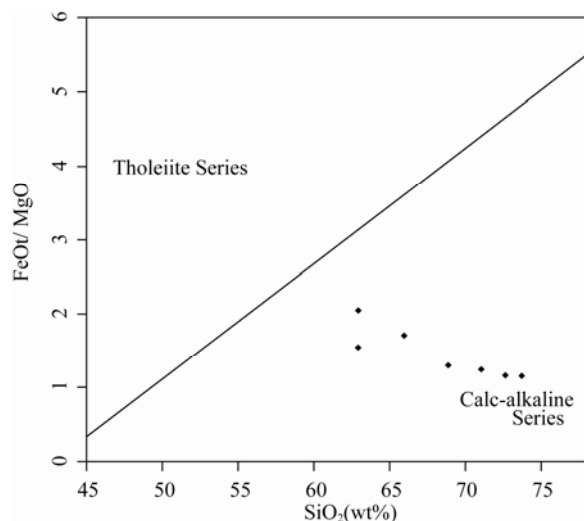


Fig. 15. The SiO_2 vs FeO/MgO plot of data points fall in calcalkaline field (after Miyashiro, 1974).

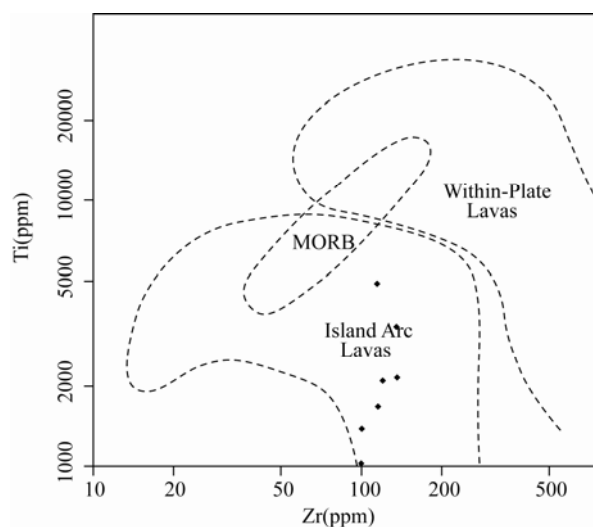


Fig. 16. The Zr vs Ti plot of data points fall in Island arc lava field which suggest convergent plate margin (after Pearce, 1982).

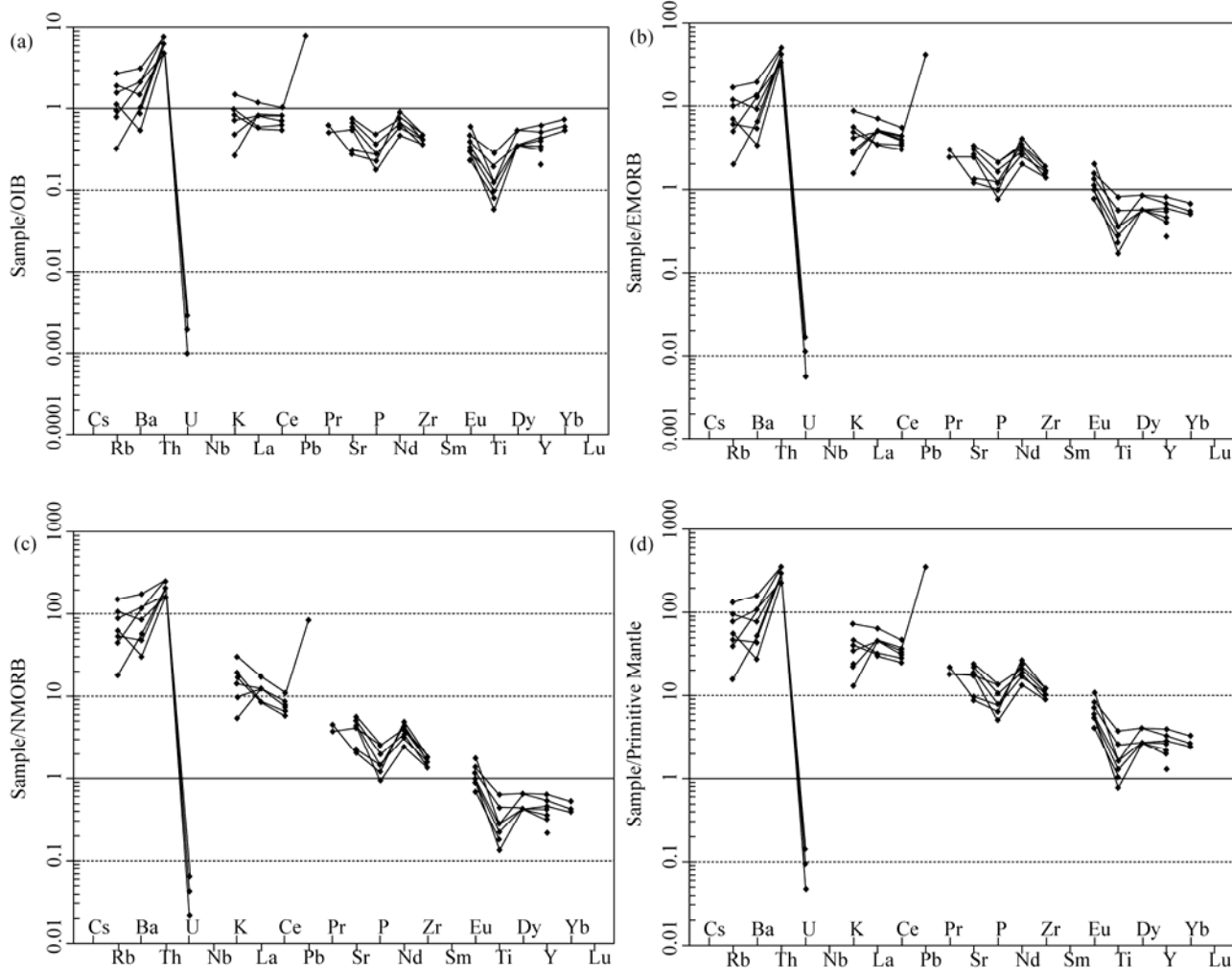


Fig 17. Spider diagrams used to demonstrate the enrichment or depletion of compatible versus incompatible elements, LREE versus HREE variation

(a), The trace element concentrations of the samples are most similar to OIB (after Sun and Mc Donough, 1989); (b), REE pattern shows similarity with E - MORB (after Sun and Mc Donough, 1989); (c), LREE and the largest LIL are enriched relative to HREE which is dissimilar to N - MORB (after Sun and Mc Donough, 1989); (d), Between 10 and 100 times more enriched in LIL and LREE compared to the primitive mantle (after Sun and Mc Donough, 1989).

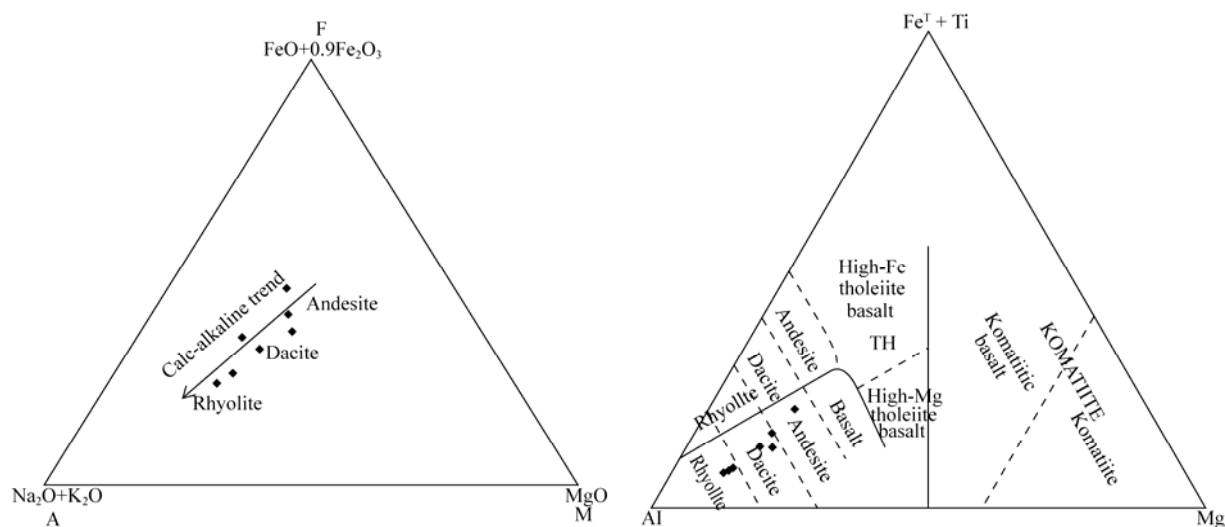


Fig. 18. AFM (A, alkali; F, iron; M, magnesium) diagram of the kadi greenstone belt rocks. The $(\text{Fe}^T + \text{Ti})$ - Al - Mg diagram (after Jansen, 1976) also supporting the AFM diagram.

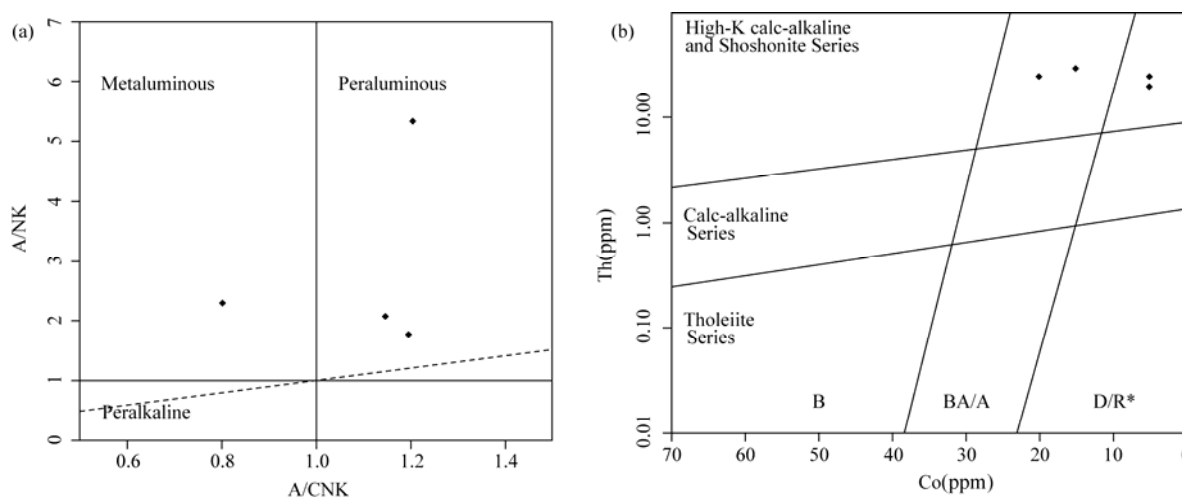


Fig. 19. (a), The A/CNK vs A/NK (mol %) plot (after Shand, 1943); (b), Th vs Co plot (after Hastie et al., 2007) shows high K calc alkaline and shoshonite series indicates late stages of ocean – continent subduction.

lowered the $P_{\text{H}_2\text{O}}$ of the magma. Then, decreased water vapor can allow silica tetrahedra to rapidly link, which can increase magma viscosity. This increase in magma viscosity may have inhibited the formation of large crystals and created a mass of hot, low density, semi-solid, fine grained material. Rhyolites formed in a continent-ocean convergent setting have high viscosity and less mobility. The uprising acidic magma along small scale linear subparallel fissures developed in the continental crust erupted forcefully and violent eruption caused brecciation of country rocks and therefore pyroclasts and lapilli were formed near the fissures. The viscous, less mobile acid lava could subsequently not move fast and blocked the pathway to create enormous pressure. With magma rising towards that surface, confining pressure would have decreased, which increases the volume of gas bubbles and decreases the density of the

magma, resulting in rapid volume expansion. After reaching the fragmentation surface, magma had changed from the liquid with suspended gas bubbles to a buoyant gaseous mixture containing liquid blobs. At that level, explosive magma rapidly propelled upward and lava erupted violently on Earth's surface. Andesites commonly occur as gray, aphanitic volcanic rock with plagioclase and rarely hornblende, pyroxene and biotite. Interestingly, the bulk composition of andesite and its plutonic equivalent diorite approximates that of terrestrial crust, suggesting that subduction zone processes have played a significant role in the development of continental crust (Hawkesworth and Kemp, 2006). The generation of voluminous andesite is favored by subduction at around a 25° angle, anatexis of thick (greater than ~ 25 km) continental, hanging wall plates and partial melting of subducted slabs at depths of 70–200 km (Gill, 1981).

Dacites are enriched in plagioclase. Minor minerals commonly include biotite, hornblende, augite, hypersthene and enstatite. Trachyandesites (as latites and shoshonites) are composed of ~66%–69% SiO_2 , although the lower TAS limit begins at 57% SiO_2 . In the Th vs Co plot (Fig. 20) after Hastie et al. (2007) the high K calc-alkaline and shoshonite series is an indicator of late stages of ocean-continent subduction. Rhyolites (> 69% SiO_2) and rhyodacites (~68–73% SiO_2) are associated with explosive silicic eruptions producing fragmental, glassy and aphanitic textures. These rocks occur as glasses, pyroclastic tuffs and breccias, or as aphanitic crystalline rocks. In addition to variations in SiO_2 , these arc rocks display significant variation in K_2O concentrations, ranging from low (tholeiitic), medium (calc-alkaline) and high K_2O (calc-alkaline to shoshonite) rock suites (Gill, 1981). The progression from tholeiite to calc-alkaline to shoshonite (trachyandesite) reflects increasing K_2O and $\text{K}_2\text{O}/\text{Na}_2\text{O}$ and decreasing iron enrichment (Jakes and White, 1972; Miyashiro, 1974).

There are a few important variables on the basis of the present data in the present context.

(1) The geochemical data shows a calc-alkaline suite of rocks whose chemistry is enriched in SiO_2 , alkalis (Na_2O and K_2O), LIL, LREE and volatiles and is relatively depleted in FeO, MgO, HFS and HREE concentrations (Miyashiro 1974; Hawkesworth et al., 1993; Pearce and Peate, 1995) like the Phanerozoic convergent margins.

(2) The $\text{Al}_2\text{O}_3/(\text{CaO}+\text{Na}_2\text{O}+\text{K}_2\text{O})$ vs. $\text{Al}_2\text{O}_3/(\text{Na}_2\text{O}+\text{K}_2\text{O})$ plot (Fig. 19a) indicates most of the data

falls under peraluminous field with acidic composition, which is indicative of ocean-continent convergence. Oceanic or thinner continental lithosphere in the overlying plate generally produces metaluminous, mafic to intermediate rocks. Thicker continental lithosphere overlying the subduction zones commonly yields peraluminous, potassic, intermediate to silicic rocks.

(3) Diversification processes such as fractionation, assimilation and magma mixing as well as metamorphic reactions strongly alter magma composition generated in the overlying wedge of the arc system. Figure 19b indicates high K calc-alkaline and shoshonite, i.e. high K andesite magma, which probably indicates melting at the base of the lithospheric stack.

(4) The old, cold, dense lithosphere favors steeply dipping subduction and young, warm, buoyant lithosphere produces shallow dipping subduction zones. The negative buoyancy of old, cold, dense ocean lithosphere is the key force driving deep lithosphere subduction in modern plate tectonics over the past 1 Ga. This negative buoyancy may not have been present in the hot, buoyant Archean ocean lithosphere such that deep subduction may not have been possible (Davies, 1992; Ernst, 2007; Stern, 2008). However, Al_2O_3 , K_2O and SiO_2 rich rhyolites, rhyodacites and shoshonites and plutonic rocks of increasingly granitic composition points to a relatively low angle subduction (~25°), thick continental lithosphere (>25 km), higher degrees of partial melting of continental lithosphere and/or arc basement, and the diminished role of ocean lithosphere subduction.

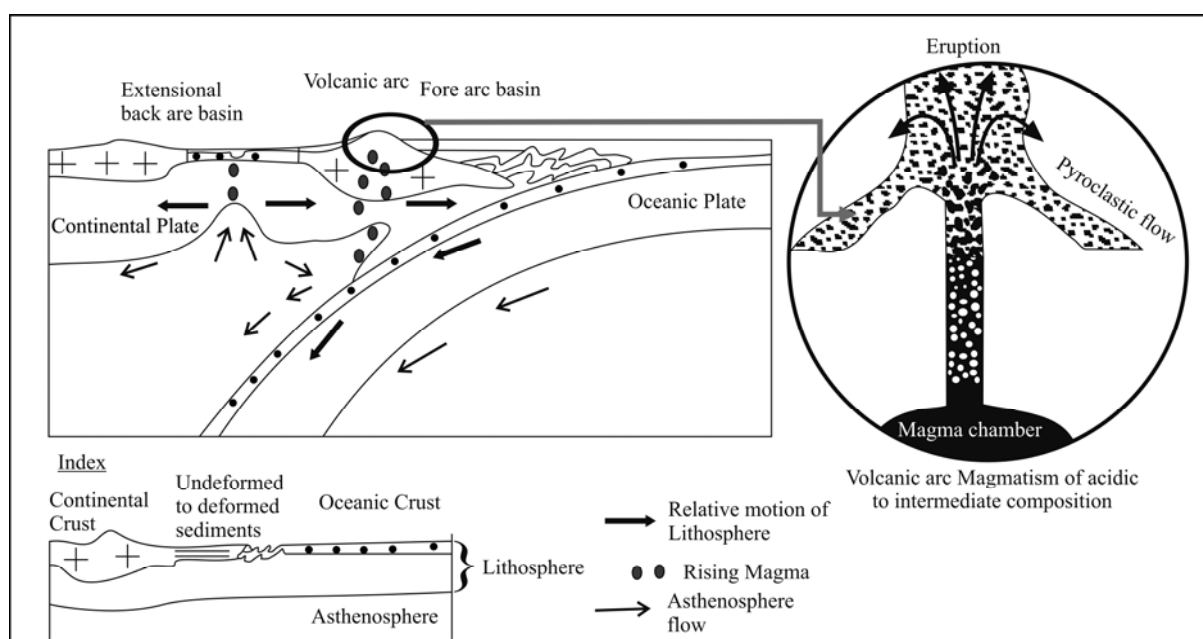


Fig. 20. Ocean - continent subduction in volcanic arc provided highly viscous acidic lava which could not move fast and blocked the fissure pathway.

(5) To generate any type of pyroclastic rock, rising and erupting magma must first be fragmented. Magmatic fragmentation is the typical process, in which coherent melt bodies rising to the surface are disrupted by the exsolution and expansion of gas (primarily H₂O and CO₂) formerly dissolved in the magma (Cashman et al., 2000). Thus, flux melting whereby volatile-rich minerals (such as micas, amphiboles, serpentine, talc, carbonates, clays and brucite) might have released H₂O, CO₂ or other volatile vapors that lowered the melting temperature of mantle rocks overlying the subduction zone. However, phreatomagmatic fragmentation also could have involved contact between magma and ground or surface waters. During magmatic fragmentation the volatile content of the magma and melt viscosity play the most important roles (Cashman et al., 2000), whereas during phreatomagmatic fragmentation, it is the external cooling media like water (Zimanowski, 1998; Morrissey et al., 2000; Zimanowski and Buettner, 2003), water-saturated sediment (White 1996), or warm hydrothermal fluids (Bertagnini et al., 1991). Any resulting pyroclasts can become remobilized, redeposited and reworked. According to Heiken and Wohletz (1986), in a single rock fragment collected during field mapping, its shape, vesicularity, and any quenching features (glass versus microlite content) may establish a phreatomagmatic fragmentation history of the melt. However, outcrop-scale studies are generally more conclusive and therefore, magmatic fragmentation is evidenced.

(6) The calc-alkaline association of basalt, andesite, dacite and rhyolite (BADR) is the signature volcanic rock suite of convergent margins and constitutes one of the most voluminous rock assemblages on Earth, second only to MORB (Perfit et al., 1980; Grove and Kinzler, 1986).

(7) Harker diagram plots of major elements generally indicate a liquid line of descent from a common source, such that BADR rocks are derived from a common parent magma of basaltic composition. The more silicic (dacite, rhyolite) members of the BADR group represent more highly fractionated daughter products.

7 Conclusion

Based on salient field observations, petrography and the discussion on the variables interpreted from the geochemical studies it can be concluded that in contrary to relatively simple decompression melting of the mantle at divergent margins, Kadiri schist belt rocks indicate convergent margin magmatism (Fig 20) which is affected by a number of variables, each of which have diversified magma composition.

Acknowledgements

The authors express sincere gratitude to Shri L. K. Nanda, Director, AMD for encouragement and logistic support to publish this part of the assigned work. The support and help extended by Dr. Syed Zakaula (RD/SR, Bangalore), Shri. A. K. Bhatt (Dy. RD/SR, Bangalore) and Shri. V. Natarajan (SO/H) are thankfully acknowledged. Special thanks to Shri. Tanmay Mukherjee, Senior Geologist, GSI for fruitful suggestions. All the fellow colleagues are sincerely acknowledged for direct and indirect supports.

Manuscript received Feb. 15, 2015

accepted Aug. 10, 2015

edited by Krisuam P. SAETHER and Fei Hongcai

References

- Bertagnini, A., Landi, P., Santacroce, R., and Sbrana, A., 1991. The 1906 eruption of Vesuvius — from magmatic to phreatomagmatic activity through the flashing of a shallow depth hydrothermal system. *B. Volcanol.*, 53(7): 517–532.
- Bowen, N.L., 1928. *The Evolution of Igneous Rocks*. Princeton University Press, Princeton NJ: 332.
- Cas, R.A.F., and Wright, J.V., 1988. Volcanic successions, modern and ancient. Chapman & Hall, London: 528.
- Cashman, K.V., Sturtevant, B., Papale, P., and Navon, O., 2000. Magmatic fragmentation; In: Sigurdsson, H. (ed.) *Encyclopedia of Volcanoes*. Academic Press, New York: 421–430.
- Chadwick, B., Vasudev, V.N., and Hegde, G.V., 2000. The Dharwar craton, southern India, interpreted as the result of late Archaean oblique convergence. *Precambrian Res.*, 99: 91–101.
- Chadwick, B., Vasudev, V., Hegde, G.V., and Nutman, A.P., 2007. Structure and SHRIMP U/Pb zircon ages of granites adjacent to the Chitradurga schist belt: implications for Neoproterozoic convergence in the Dharwar craton, southern India. *J. Geol. Soc. India*, 69: 5–24.
- Chardon, D., and Jayananda, M., 2008. Three-dimensional field perspective on deformation, flow, and growth of the lower continental crust (Dharwar craton, India). *Tectonics*, 27 TC1014, <http://dx.doi.org/10.1029/2007TC002120>.
- Chardon, D., Jayananda, M., and Peucat, J.J., 2011. Lateral constrictional flow of hot orogenic crust: insights from the Neoproterozoic of South India, geological and geophysical implications for orogenic plateaux. *Geochemistry, Geophysics, Geosystems*, 12 Q02005, <http://dx.doi.org/10.1029/2010GC003398>.
- Davies, G.F., 1992. On the emergence of plate tectonics. *Geology*, 20: 963–966.
- Dey, S., Nandy, J., Choudhary, A.K., Liu, Y., Zong, K., 2014. Origin and evolution of granitoids associated with the Kadiri greenstone belt, eastern Dharwar craton: A history of orogenic to anorogenic magmatism. *Precambrian Research*, 246: 64–90.
- Drury, S.A., and Holt, R.W., 1980. The tectonic framework of the south Indian craton: a reconnaissance involving

- LANDSAT imagery. *Tectonophysics*, 65: 71–75.
- Ernst, W.G., 2007. Speculations on evolution of the terrestrial lithosphere – asthenosphere system – plumes and plates. *Gondwana Res.*, 11: 38–49.
- Fisher, R.V., and Schmincke, H.U., 1984. *Pyroclastic Rocks*. Heidelberg, Springer: 474.
- Gill, J.B., 1981. *Orogenic Andesites and Plate Tectonics*. Springer - Verlag, New York: 390.
- Goodwin, A.M., Ambrose, J.W., Ayres, L.D. et al., 1972. The Superior Province. *Geol. Ass. Canada Spec Paper*, 11: 527–624.
- Goswami, S., Sivasubramaniam, R., Bhagat, S., Suresh, K., and Sarbajna, C., 2016. Algoma type BIF and associated submarine volcano-sedimentary sequence in Ramagiri granite-greenstone terrain, Andhra Pradesh, India. *Journal of Applied Geochemistry*, 18(2): 155–169.
- Grove, T.L., and Kinzler, R.J., 1986. Petrogenesis of andesites. *Annu. Rev. Earth. Pl. Sc.*, 14: 417–454.
- Harker, A., 1909. *The Natural History of Igneous Rocks*. McMillan Publishers, New York: 384.
- Hastie, A.R., Kerr, A.C., Pearce, J.A., and Mitchell, S.F., 2007. Classification of altered volcanic island arc rocks using immobile trace elements: development of the Th, Co discrimination diagram. *Journal Petrology*, 48: 2341–2357.
- Hawkesworth, C.J., Gallagher, K., Hergt, J.M., Keynes, M., 1993. Mantle and slab contributions in arc magmas. *Annu. Rev. Earth Pl. Sc.*, 21: 175–204.
- Hawkesworth, C.J., and Kemp, A.I.S., 2006. Evolution of the continental crust. *Nature*, 443: 811–817.
- Heiken, G.H., and Wohletz, K.H., 1986. *Volcanic Ash*. Berkeley, University of California Press: 246.
- Ishikawa, Y., Sawaguchi, T., Iwaya, S., and Horiuchi, M., 1976. Delineation of prospecting targets for Kuroko deposits based on modes of volcanism of underlying dacite and alteration halos. *Mining Geology*, 26: 105–117 (in Japanese with English abs.).
- Jakes, P., and White, A.J.R., 1972. Major and trace element abundances in volcanic rocks of orogenic areas. *B. Geol. Soc. America*, 83: 29–40.
- Jayananda, M., Chardon, D., Peucat, J.J., Capdevila, R., and Martin, H., 2006. 2.61 Ga potassic granites and crustal reworking, western Dharwar craton (India): tectonic, geochronologic and geochemical constraints. *Precambrian Research*, 150: 1–26.
- Jayananda, M., Peucat, J.J., Chardon, D., Krishna Rao, B., Fanning, C.M., and Corfu, F., 2013. Neoproterozoic greenstone volcanism and continental growth, Dharwar craton, southern India: Constraints from SIMS U–Pb zircon geochronology and Nd isotopes. *Precambrian Research*, 227: 55–76.
- Jensen, L.S., 1976. A New Cation Plot for Classifying Subalkalic Volcanic Rocks. *Ontario Geol. Surv. Misc. Paper*: 66.
- McPhie, J., Doyle, M., and Allen, R., 1993. *Volcanic Textures. A guide to the interpretation of textures in volcanic rocks*. Tasmania, Tasmanian Government Printing Office: 196.
- Miyashiro, A., 1974. Volcanic rock series in island arcs and active continental margins. *Am. J. Sci.*, 274: 321–355.
- Morrissey, M.M., Zimanowski, B., Wohletz, K., and Büttner, R., 2000. Phreatomagmatic fragmentation; In: Sigurdsson, H., Houghton, B.F., McNutt, S.R., Rymer, H., and Stix, J. (eds.), *Encyclopedia of Volcanoes*. New York, Academic Press: 431–446.
- Nandy, J., and Dey, S., 2013. The mechanism of Neoproterozoic granitoid formation: Evidence from eastern Dharwar Craton, Southern India. *Am. Int. J. Res. Formal, Appl. Natural Sci. (AIJRFANS)*, 3(1): 105–109.
- Pearce, J.A., 1982. Trace element characteristics of lavas from destructive plate boundaries; In: Thorpe, R.S. (ed.), *Andesites: Orogenic Andesites and Related Rocks*. John Wiley & Sons, Chichester: 525–548, ISBN 0 471 28034 8.
- Pearce, J.A., and Peate, D.W., 1995. Tectonic implications of the composition of volcanic arc magmas. *Annu. Rev. Earth. Pl. Sc.*, 23: 251–285.
- Perfit, M.R., Gust, D.A., Bence, A.E., Arculus, R.J., and Taylor, S.R., 1980. Chemical characteristics of island - arc basalts: implications for mantle sources. *Chemical Geology*, 30: 227–256.
- Shand, S.J., 1943. *Eruptive Rocks. Their Genesis, Composition, Classification, and Their Relation to Ore-Deposits with a Chapter on Meteorite*. New York: John Wiley & Sons.
- Shan Houxiang, Zhai Mingguo and Dey Sukanta, 2016. Petrogenesis of two types of Archean TTGs in the North China Craton: a case study of intercalated TTGs in Lushan and non-intercalated TTGs in Hengshan. *Acta Geologica Sinica* (English Edition), 90(6): 2049–2065.
- Sreenivasulu, P., Padmasree, P., and Hanumanthu, P.C., 2014. Granitoids adjoining Kadiri schist belt, Andhra Pradesh, South India: Field and petrographic implications. *International Journal of Geology, Earth. Env. Sc.*, 4: 244–258.
- Stern, R.J., 2008. Modern style plate tectonics began in Neoproterozoic time: an alternative interpretation of Earth's tectonic history; In: Condie, K.C., and Pease, V. (eds.), *When Did Plate Tectonics Begin on Planet Earth?* Geol. Soc. America Spec. Paper, 440: 265–280.
- Sun, S., and McDonough, W.F., 1989. Chemical and isotopic systematics of oceanic basalts: implications for mantle composition and processes. In: Saunders, A.D., and Norry, M.J. (eds.), *Magma-tism in Ocean Basins*. Blackwell Scientific, Boston: 313–345.
- White, J.D.L., 1996. Impure coolants and interaction dynamics of phreatomagmatic eruptions. *J. Volcanol. Geoth. Res.*, 65: 1–17.
- Wohletz, K.H., and McQueen, R.G., 1984. Volcanic and stratospheric dust like particles produced by experimental water-melt interactions. *Geology*, 12(10): 591–594.
- Zimanowski, B., 1998. Phreatomagmatic explosions. In: Freundt, A., and Rosi, M. (eds.), *From magma to tephra*. Amsterdam, Elsevier, Dev. Volcanol., 4: 25–53.
- Zimanowski, B., and Buettner, R., 2003. Phreatomagmatic explosions in subaqueous volcanism; In: White, J.D.L., Smellie, J.L., and Clague, D.A. (eds.), *Explosive subaqueous volcanism; Geophysical Monographs*. Washington D.C., American Geophysical Union: 51–60.

Brief introduction to the first author:

Sukanta GOSWAMI is a professional exploration geologist of Department of Atomic Energy. He is post graduated in 2009 in applied geology from Presidency College, Kolkata, India and completed M. Tech (2014) in exploration geosciences from Homi Bhabha National Institute, India.